Journal for Geometry and Graphics
Volume 16 (2012), No. 1, 47–58.

# On Some Surfaces in Kinematics

**Manfred Husty**

*Institute for Basic Sciences in Engineering, Unit Geometry and CAD*
*University Innsbruck, Technikerstr. 13, 6020 Innsbruck, Austria*
*email: manfred.husty@uibk.ac.at*

**Abstract.** This paper presents a collection of geometrically interesting results obtained within the last years in kinematic contexts. Special emphasis is laid on geometric objects that describe kinematic features like workspaces or singularities of robots and mechanisms.

*Key Words:* Kinematics, kinematic features, surfaces, kinematic mapping, workspace, singularity.

*MSC 2010:* 53A17, 51N05

## 1. Introduction

Kinematic mapping of planar, spherical or spatial kinematics uses three or seven dimensional parameter spaces to represent motions or displacements. Algebraic varieties in these spaces encode kinematic properties of mechanisms or robots. Geometric properties of the varieties in the image spaces provide insight into the motions in the Cartesian spaces. Kinematic image spaces as they have been introduced by geometricians like Study [20], Blaschke [1] or Grünwald [9] are point models of Euclidean displacements but they are not the only parameter spaces that can be used to represent displacements. There are other parameter spaces in which kinematic features sometimes are better represented, like e.g. joint spaces of mechanisms. Each representation has its advantages and disadvantages. It is interesting to observe that the same kinematic feature can be represented by geometrically very different surfaces. From this follows that there exist interesting maps between these different spaces. Without going into computational details, some surfaces and the corresponding kinematic features are discussed. But to the best of the author's knowledge the presented algorithm to compute the workspace of a regional 3-$R$ manipulator is new and shows how geometric considerations simplify the computations up to a level that the equations can be presented in complete generality.

This paper is organized as follows: In Section 2 we briefly recall Study's kinematic mapping, in Section 3 geometric objects which represent workspaces of manipulators are introduced and in Section 4 geometric objects which encode kinematic properties in are presented.

ISSN 1433-8157/\$ 2.50 

## 2. Study's kinematic mapping

Euclidean three space is the three dimensional real vector space $\mathbb{R}^3$ together with the usual scalar product $\mathbf{x}^T\mathbf{y} = \sum_{i=1}^3 x_i y_i$. A Euclidean displacement is a mapping

$$\gamma\colon \mathbb{R}^3 \to \mathbb{R}^3, \quad \mathbf{x} \mapsto \mathbf{A}\mathbf{x} + \mathbf{a} \tag{1}$$

where $\mathbf{A}$ is a proper orthogonal three by three matrix and $\mathbf{a} \in \mathbb{R}^3$ is a vector. The entries of $\mathbf{A}$ fulfill the well-known orthogonality condition $\mathbf{A}^T \cdot \mathbf{A} = \mathbf{I}_3$, where $\mathbf{I}_3$ is the three by three identity matrix.

The group of all Euclidean displacements is denoted by SE(3). It is a convenient convention to write (1) as product of a four by four matrix and a four dimensional vector according to

$$\begin{bmatrix} 1 \\ \mathbf{x} \end{bmatrix} \mapsto \begin{bmatrix} 1 & \mathbf{o}^T \\ \mathbf{a} & \mathbf{A} \end{bmatrix} \cdot \begin{bmatrix} 1 \\ \mathbf{x} \end{bmatrix}. \tag{2}$$

Study's kinematic mapping $\varkappa$ maps an element $\alpha$ of SE(3) to a point $\mathbf{x} \in P^7$. If the homogeneous coordinate vector of $\mathbf{x}$ is $[x_0 : x_1 : x_2 : x_3 : y_0 : y_1 : y_2 : y_3]^T$, the kinematic pre-image of $\mathbf{x}$ is the displacement $\alpha$ described by the transformation matrix

$$\frac{1}{\Delta} \begin{bmatrix} x_0^2+x_1^2+x_2^2+x_3^2 & 0 & 0 & 0 \\ p & x_0^2+x_1^2-x_2^2-x_3^2 & 2(x_1x_2-x_0x_3) & 2(x_1x_3+x_0x_2) \\ q & 2(x_1x_2+x_0x_3) & x_0^2-x_1^2+x_2^2-x_3^2 & 2(x_2x_3-x_0x_1) \\ r & 2(x_1x_3-x_0x_2) & 2(x_2x_3+x_0x_1) & x_0^2-x_1^2-x_2^2+x_3^2 \end{bmatrix} \tag{3}$$

where

$$\begin{aligned} p &= 2(-x_0y_1 + x_1y_0 - x_2y_3 + x_3y_2), \\ q &= 2(-x_0y_2 + x_1y_3 + x_2y_0 - x_3y_1), \\ r &= 2(-x_0y_3 - x_1y_2 + x_2y_1 + x_3y_0), \end{aligned} \tag{4}$$

and $\Delta = x_0^2 + x_1^2 + x_2^2 + x_3^2$. The matrix operator in (3) describes an element of SE(3) if

$$x_0y_0 + x_1y_1 + x_2y_2 + x_3y_3 = 0 \tag{5}$$

holds and not all $x_i$ are zero. If these conditions are fulfilled we call $[x_0 : \cdots : y_3]^T$ the *Study parameters* of the displacement $\alpha$. The important relation (5) defines a quadric $S_6^2 \subset P^7$ and the range of $\varkappa$ is this quadric minus the three dimensional subspace defined by

$$E\colon x_0 = x_1 = x_2 = x_3 = 0. \tag{6}$$

We call $S_6^2$ the *Study quadric* and $E$ the *exceptional* or *absolute generator*[1].

The restriction of Study's kinematic mapping to certain three-spaces on the Study quadric yields two important subgroups of SE(3), the group of planar Euclidean displacements SE(2) and the special orthogonal group SO(3) whose elements are pure rotations without any translational component. Both groups are of relevance in kinematics. The planar Euclidean motion group SE(2) can be embedded into SE(3) by substituting $x_2 = x_3 = y_0 = y_1 = 0$ into (3). This yields the matrix parameterization

$$\frac{1}{x_0^2+x_1^2} \begin{bmatrix} x_0^2+x_1^2 & 0 & 0 \\ 2(-x_0y_2+x_1y_3) & x_0^2-x_1^2 & -2x_0x_1 \\ 2(-x_0y_3-x_1y_2) & 2x_0x_1 & x_0^2-x_1^2 \end{bmatrix} \tag{7}$$

[1] A more detailed introduction to kinematic mapping can be found in [13].

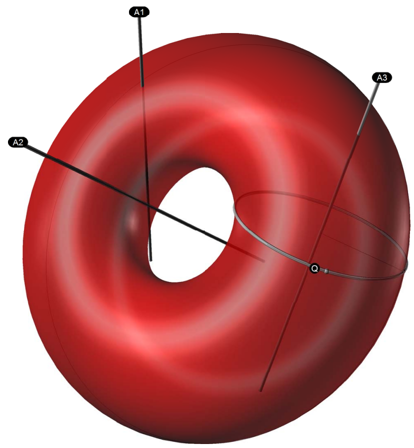


Figure 1: Surface of revolution generated by rotations about axes $a_2$ and $a_3$

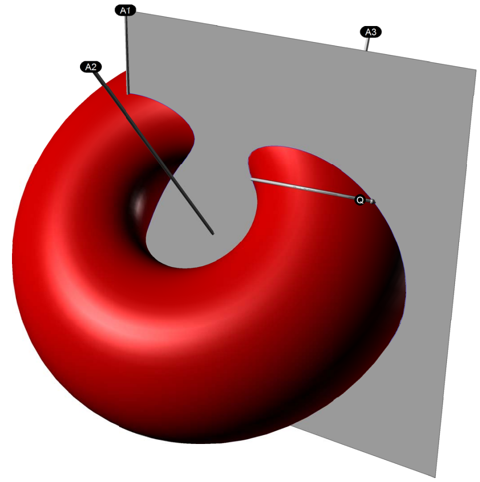


Figure 2: Cross-section plane intersecting in a curve of the two-parameter family (9)

of SE(2) (the second row and the second column in (3) were omitted). The group SE(2) can be considered as kinematic pre-image of the three space $x_2 = x_3 = y_0 = y_1 = 0$, minus its intersection with the exceptional generator $E$, which is a line. We identify this three space with $P^3$ and describe its points by homogeneous coordinates $[x_0 : x_1 : y_2 : y_3]^T$. The geometry of $P^3$ as range of planar kinematic mapping is governed by a change of coordinates in the moving or fixed frame of the planar displacements or, equivalently, by a Cayley-Klein geometry with the absolute figure consisting of the line $x_0 = x_1 = 0$ and the absolute points $[0 : 0 : 1 : \pm\mathrm{i}]^T$ This geometry is called *quasielliptic* [4, p. 399].

The spherical motion group SO(3) can be embedded in SE(3) via the matrix operator

$$\frac{1}{\Delta}\begin{bmatrix} x_0^2+x_1^2-x_2^2-x_3^2 & 2(x_1x_2-x_0x_3) & 2(x_1x_3+x_0x_2) \\ 2(x_1x_2+x_0x_3) & x_0^2-x_1^2+x_2^2-x_3^2 & 2(x_2x_3-x_0x_1) \\ 2(x_1x_3-x_0x_2) & 2(x_2x_3+x_0x_1) & x_0^2-x_1^2-x_2^2+x_3^2 \end{bmatrix} \tag{8}$$

where $\Delta = x_0^2 + x_1^2 + x_2^2 + x_3^2$. It is the kinematic pre-image of the three space $y_0 = y_1 = y_2 = y_3 = 0$. The absolute figure is the exceptional quadric $y_0^2 + y_1^2 + y_2^2 + y_3^2 = 0$ and the corresponding geometry is *elliptic* [2].

## 3. Workspaces of mechanisms and robots

The workspace of a mechanism is the set of all poses (= positions and orientations) the endeffector of the device can reach. In terms of kinematic mapping this means: the workspace is the set of all points in the image space that correspond to endeffector poses. But there are many other different definitions for the workspace. Very often only one point in the endeffector frame is considered, which results in neglecting the orientation of the frame and then the workspace becomes some solid in 3D Cartesian space. There is also a fundamental difference between the workspaces of parallel or serial robots. We will show this with two very simple, but prototypical manipulators, the planar 3-$RPR$ parallel robot and the regional 3-$R$ serial manipulator, where a revolute joint is denoted by $R$ and a prismatic joint is denoted by $P$. In case of the serial 3-$R$ chain the workspace of a point $Q$ in the end effector frame is generated by a one parameter sweep of a surface of revolution. This surface of revolution is obtained when the point $Q$ is rotated about the third axis $A3$, which yields a circle and this circle is rotated about the second axis $A2$. These two rotations produce therefore a surface of revolution (see Fig. 1), which itself generates the whole workspace when it is rotated about the first axis $A1$. The boundary of the workspace is again a surface of revolution which can be obtained by an approach due to M. Ceccarelli [5]:

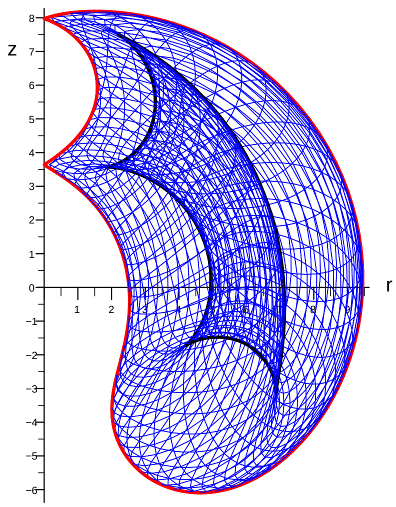


Figure 3: Two-parameter set of curves in the cross section of the workspace

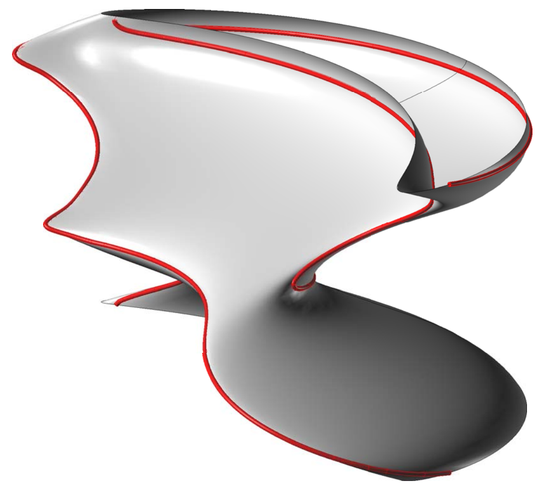

Figure 4: Graph of the level set

The workspace boundary of a general 3-$R$ manipulator can be expressed as function of radial and axial reaches, $r$ and $z$ respectively, with respect to the base frame. The reaches $r$ and $z$ can be evaluated as functions of coordinates of the position vectors in the form

$$r_0 = (H_0^x)^2 + (H_0^y)^2 = (H_1^x \cos\theta_1 - H_1^y \sin\theta_1)^2 + (H_1^x \sin\theta_1 + H_1^y \cos\theta_1)^2, \quad z_0 = H_0^z,$$

which can be equivalently expressed in the form

$$r = (H_1^x)^2 + (H_1^y)^2, \quad z = H_1^z, \tag{9}$$

in which $H_i$ are the components of the position vector of the end-effector point with respect to reference frame $i$, $\theta_1$ is the rotation angle about the first axis and $r, z$ are the coordinates of a conveniently chosen cross-section plane passing through the first axis (Fig. 2). Because $H_1$ is a function of the two rotation angles $\theta_2$ and $\theta_3$ of the rotations about the second and the third axis, (9) represents a 2-parameter family of curves. Its envelope is the cross-section workspace contour in the cross-section plane. It is a function of the Denavit-Hartenberg (DH) parameters and can be used to express the vector components $H_1^x, H_1^y$ and $H_1^z$ in the form of a so called ring equation [5]. This two-parameter set can also be interpreted as a level set with one parameter set of curves as level sets of the other parameter. When one uses one of the two angles of rotation (e.g $\theta_3$) as the parameter of the pencil of curves then one can generate the graph of this level set (Fig. 4). In [15] and [16] it was shown that this surface, after algebraization of the rotation angles is of degree 12. It is interesting to note that the boundary of the two-parameter set of curves in (9) (thick red curve in Fig. 3) corresponds to the singularities in the displayed meridian plane of the workspace solid. This curve is on the other hand the orthogonal projection of the contour of the graph of the level set surface (thick red curve in Fig. 4) into the level set plane[2].

A second approach to derive the workspace boundaries is based on a very geometric observation: The operation point $Q$ is on the boundary iff there is a line $l$ passing through $Q$ and intersecting all three axes (Fig. 5). From kinematic point of view the boundary characterizes the singular positions of the operation point, because the operation point cannot move in the direction of $l$. On the other hand one can use this line condition to characterize all points in the end-effector space which are at a certain instant in a singular position: these points are on the hyperboloid which is determined by the three axes $A1, A2, A3$.

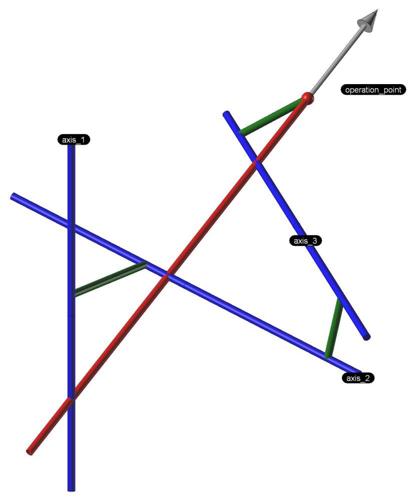


Figure 5: Singular position of the operation point

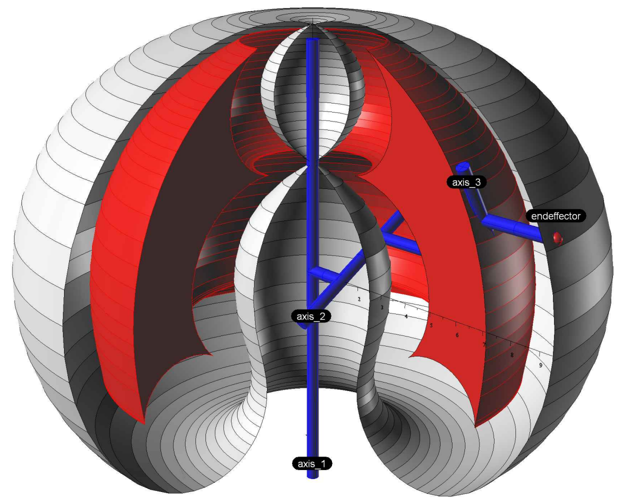


Figure 6: Workspace boundaries of 3-$R$ manipulator

With this geometric insight it is straightforward to derive the boundary condition: In a first step the equation of the plane $\varepsilon$ spanned by the axis $A1$ and the operation point $Q$ is derived. Then the two piercing points $P_1$ and $P_2$ of the axes $A_2$ and $A_3$ with $\varepsilon$ are determined. The boundary condition $B$ is given by the collinearity condition of the three points $P_1, P_2, Q$. This condition can be derived completely general (i.e. without specifying the DH-parameters)

$$\begin{aligned}
B:\ \cos\theta_3^2 &\left[a_3\sin\theta_2(a_2\sin\alpha_1\cos\alpha_2 - a_1\cos\alpha_1\sin\alpha_2) + a_3d_2\cos\theta_2\sin\alpha_2\sin\alpha_1\right]\\
&+\cos\theta_3\sin\theta_3\left[-a_3(a_1\cos\alpha_1\sin\alpha_2\cos\alpha_2 - \sin\alpha_1 a_2)\cos\theta_2\right.\\
&\left.-a_3\sin\alpha_1(a_1\cos\alpha_2^2 + \sin\theta_2\sin\alpha_2 d_2\cos\alpha_2 - a_1)\right]\\
&+\cos\theta_3\left[(-a_1\cos\alpha_1 d_3 + \sin\alpha_1 a_2\sin\alpha_2 d_2 + a_1\cos\alpha_1 d_3\cos\alpha_2^2)\cos\theta_2\right.\\
&\left.+(-a_1a_2\cos\alpha_1\sin\alpha_2 - d_3\sin\alpha_1 d_2 + \cos\alpha_2^2 d_3\sin\alpha_1 d_2)\sin\theta_2 - \sin\alpha_1 d_3 a_1\sin\alpha_2\cos\alpha_2\right]\\
&+a_2\sin\alpha_1\sin\theta_3(a_2\cos\theta_2 - d_3\sin\theta_2\sin\alpha_2 + a_1) - a_2a_3\cos\alpha_2\sin\theta_2\sin\alpha_1 = 0,
\end{aligned} \tag{10}$$

where $\alpha_1,\ d_2,\ a_1, \alpha_2,\ d_3,\ a_2$ denote the DH-parameters encoding the angle and the distance between two axes and the offset (see [19]). $B$ is linear in $\sin\theta_2$ and $\cos\theta_2$ and therefore quadratic in algebraic parameters $u$ ($\cos\theta_2 = \frac{1-u^2}{1+u^2}, \sin\theta_2 = \frac{2u}{1+u^2}$). A parametric expression for the boundary curve is found by solving $B$ for $u$ and substituting into (9). An implicit

[2]All figures are in color that can be seen in the web version of the paper.

equation of the boundary curve is computed after algebraization of $\theta_2$ and $\theta_3$ and elimination of both algebraic parameters from $B, r$ and $z$ of (9). The result is that the boundary curve is an algebraic curve of degree 16, which is symmetric with respect to the first axis. If this curve is rotated about the first axis, a revolute surface of degree 16 is obtained. Fig. 6 shows the workspace boundaries of an example manipulator with DH-parameters $\alpha_1 = \pi/3$, $\alpha_2 = \pi/2$, $a_1 = 13/10$, $a_2 = 5$, $a_3 = 5/2$, $d_2 = 21/10$, $d_3 = -23/10$. The two boundary surfaces have the following kinematic meaning: If the operation point is in the inner (red) solid the inverse kinematics has four solutions (there are four possible configurations of the axes to reach the point), outside of the red solid the inverse kinematics has two solutions.

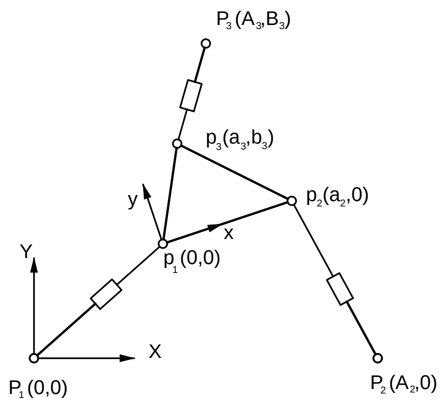


Figure 7: Planar 3-$RPR$ parallel manipulator

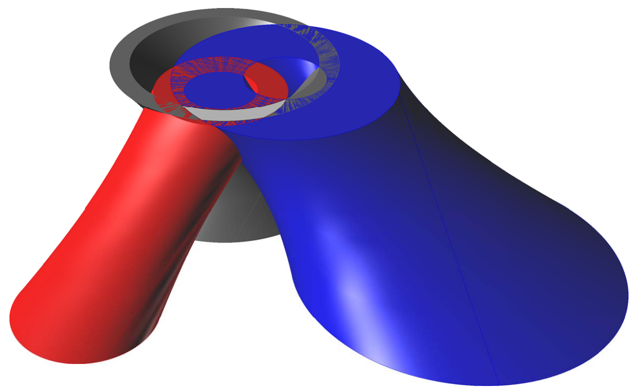

Figure 8: Workspace of a 3-RPR manipulator

Workspaces of parallel manipulators are quite different. They consist of the intersection of the workspaces of all of their kinematic chains. We will discuss this feature here presenting a simple planar manipulator, the 3-$RPR$ manipulator (Fig. 7). This manipulator is the planar equivalent to the famous Gough-Stewart platform which is practically used, for example, as flight simulator mechanism. This manipulator consists of a moving plate connected to the fixed base via three extensible legs mounted to base and platform with revolute joints. The end-effector plate moves freely within the plane when three prismatic joints, which extend the legs, are actuated. If the actuated joint parameters are unlimited, the possible poses cover the whole plane with all possible orientations. Practically this is of course not the case. There will be a maximum and a minimum extension of the prismatic joints. As mentioned above the workspace will be the intersection of the three workspaces of each leg of the manipulator. Therefore we discuss at first the workspace of one leg, i.e. a serial $RPR$-chain. If the $P$ joint is locked then the chain has two rotational degrees of freedom, the set of end-effector poses in the kinematic image space is two parametric, a surface. This surface represents the only mechanical constraint which is posed on the mechanism when the P joint is locked: the center of the revolute on the moving platform is bound to move on a circle. After a change of coordinates in the image space (7) and renaming $y_2 = x_3, y_3 = -x_2, x_1 = -x_1, x_0 = -x_0$ the equation of this surface can be computed as:

$$\begin{aligned}\Big(x_2 - \frac{1}{2}\big(c_2 + C_2 - x_1(C_1 - c_1)\big)\Big)^2 + \Big(x_3 - \frac{1}{2}\big(x_1(c_2 - C_2) - C_1 - c_1\big)\Big)^2 \\ - \frac{1}{4}\,R^2\,(x_1^2 + 1) \;=\; 0.\end{aligned} \tag{11}$$

This equation represents the circle constraint for a general leg with base center $(C_1, C_2)$ and moving center $(c_1, c_2)$. The equations for the three legs can be obtained in a simplified form when the coordinate system is specially adapted (see Fig. 7). Substituting the coordinates of the fixed and moving pivots of the manipulator Fig. 7 into the constraint equation we obtain three equations:

$$\begin{aligned}
h_1 &: \ 4x_2^2 + R_1 + 4x_3^2 = 0 \\
h_2 &: \ 4x_2^2 + R_2 - 4A_2x_3x_0 + 4x_3x_0a_2 + 4x_3^2 - 4x_1x_2a_2 - 4x_1A_2x_2 \\
&\quad + 4x_1^2A_2a_2 - 2A_2a_2 = 0 \\
h_3 &: \ 4x_2^2 + 4B_3x_0x_2 + R_3 - 4A_3x_3x_0 - 4x_2x_0b_3 + 4x_3x_0a_3 + 4x_3^2 \\
&\quad - 4x_1B_3x_0a_3 + 4x_1A_3x_0b_3 - 4x_1x_2a_3 - 4x_1B_3x_3 - 4x_1A_3x_2 \\
&\quad - 4x_1x_3b_3 + 4x_1^2A_3a_3 + 4x_1^2B_3b_3 - 2B_3b_3 - 2A_3a_3 = 0.
\end{aligned} \tag{12}$$

These equations represent hyperboloids in the kinematic image space. When the prismatic joint is in its maximum extension we obtain a hyperboloid $h_{imax}$ and when the leg is at its minimum extension we again obtain a hyperboloid $h_{imin}$. The sought workspace lies between these two surfaces and can be obtained by computing the difference of two solids $Sh_{imax} - Sh_{imin}$. For the whole mechanism there are six hyperboloids and therefore three solids. The workspace can be found by the intersection of the three solids corresponding to the three legs. The workspace of a generic manipulator of this type is displayed in Fig. 8 (see also [10]).

When spatial parallel manipulators are discussed then the workspace question becomes much more involved. The spatial equivalent to the planar parallel manipulator discussed above is the Gough-Stewart platform. A Gough-Stewart platform is a parallel manipulator, which consists of a mobile platform connected to a base via six linearly actuated links (legs). The links are mounted to the platform with spherical and to the base with universal joints. This manipulator provides six degrees of freedom within a well defined workspace. The workspace is a six-dimensional solid in the kinematic image space. Only if one restricts to either constant orientation or constant position, then the corresponding workspaces can be displayed. In case of constant orientation the workspace of a Gough-Stewart platform is the intersection of six solids. Each of the solids is obtained by the difference of a maximum sphere of the extension of one leg and the minimum sphere of the minimum extension of the same leg. Both spheres are centered at the same point, which is the center of the base universal joint. Fig. 9 shows a model of a Gough-Stewart platform with the workspace of the origin $C$ of the moving coordinate system $(x-y-z)$ corresponding to an orientation when the platform stays parallel to the base and does not rotate. In [17] and [18] interesting possibilities are shown to overcome the dimensional difficulties in displaying the workspaces of complicated spatial parallel manipulators.

## 4. Kinematic properties

Singularities are kinematic features of special interest. In case of a serial manipulator the device looses at least one degree of freedom in a singularity. In case of a parallel manipulator it gains at least one degree of freedom in a singular pose. Both cases are unwanted in practical work because they mean that the operator looses control or that motors might break. The description of singularities is therefore an important task in the kinematic analysis but equally important in the synthesis of mechanisms. The discussion of singularities of serial manipulators is closely related to line geometry and subvarieties of lines (see [19]). We confine ourselves in this paper to singularities of parallel manipulators and discuss especially

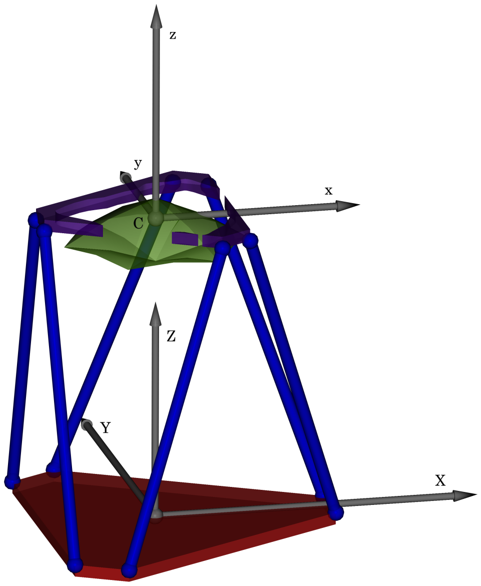


Figure 9: Workspace of Gough-Stewart platform

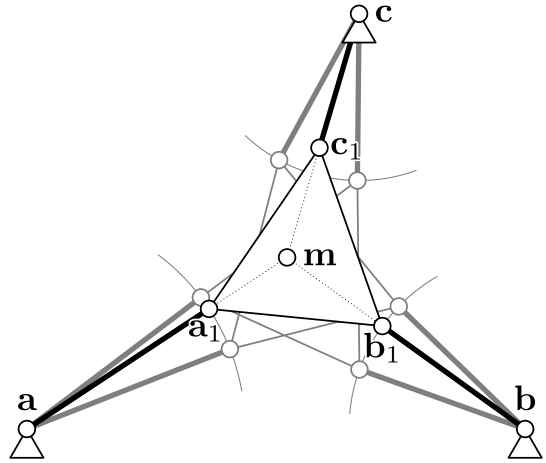


Figure 10: Singular pose of a planar 3-$RPR$ manipulator

the singularities of the 3-$RPR$ planar parallel manipulator. When a parallel manipulator is described by a set of algebraic equations as for example in (12) then we can discuss more generally the algebraic variety $V \in P^7$ determined by a set of such equations. Let $p = [p_0, \ldots, p_7]^T$ be a point on $V$. The *tangent space* of $V$ at $p$, denoted $T_p(V)$, is the variety

$$T_P(V) = \mathbf{V}(d_p(f))\colon f \subset \mathbf{I}(\mathbf{V}) \tag{13}$$

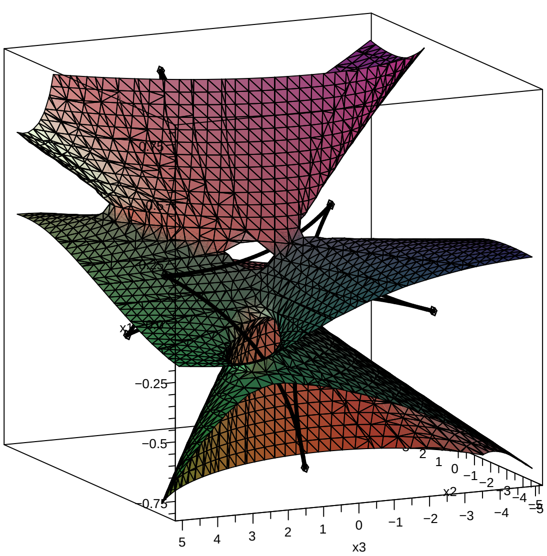


Figure 11: Singularity surface of a planar 3-$RPR$ manipulator in kinematic image space

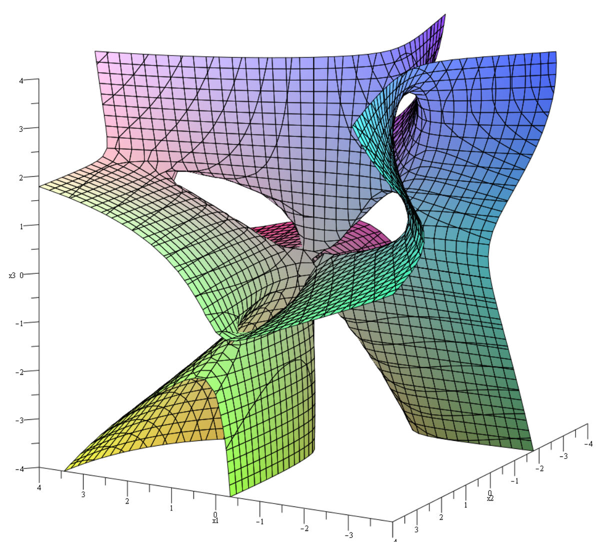

Figure 12: Singularity surface of spherical 3-$RPR$ manipulator

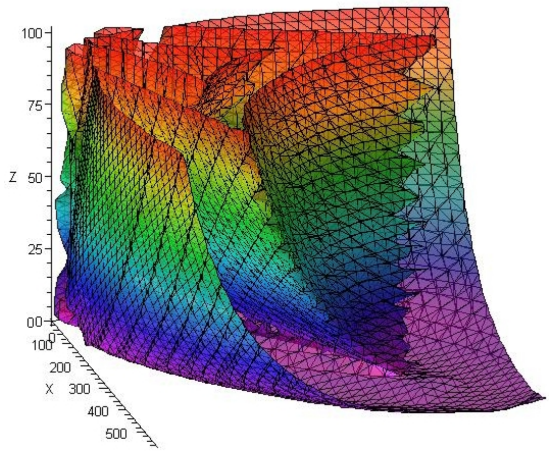


Figure 13: Singularity surface of a planar 3-$RPR$ manipulator in joint space

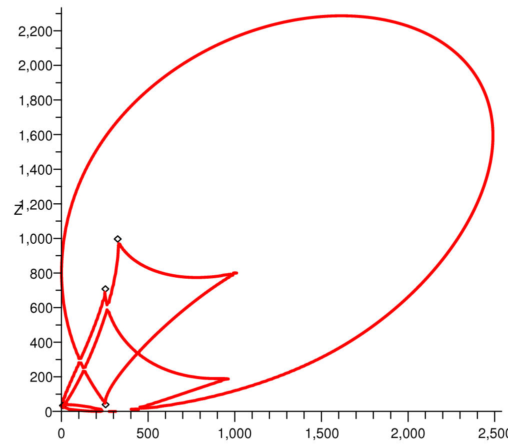


Figure 14: Horizontal cross-section of the singularity surface in joint space

of linear forms of all polynomials contained in the ideal $\mathbf{I(V)}$ in point $p$ (see [7, p. 486]). With this definition we can immediately link the tangent space to the local degree of freedom of the mechanism: The local degree of freedom is defined as $\dim T_p(V)$. In case of a general 6-$R$ serial manipulator the dimension of the tangent space should be six, meaning that the manipulator is free to move in any direction and orientation. In a singularity this motion capability is restricted in one, two or more dimensions depending on the rank of the Jacobian of the system of equations. In case of a general six degrees of freedom (6-dof) parallel manipulator the dimension of the tangent space is given by the intersection of six fully dimensional tangent spaces of each leg and therefore should be zero. If the manipulator is in a singular pose than the intersection of the six tangent spaces is one, two or more dimensional and the manipulator gains one, two or more degrees of freedom and becomes locally unstable. Computationally the differentials are to be taken with respect to the Study parameters $x_i, y_i$. In kinematics these differentials are collected in the *Jacobian matrix* of the manipulator

$$\mathbf{J}(f_j) = \left(\frac{\partial f_j}{x_i}, \frac{\partial f_j}{y_i}\right), \tag{14}$$

where $f_j$ are polynomials describing the constraints, the Study condition, and a normalizing condition. The normalizing condition has to be added to avoid dimensional problems coming from the exceptional generator $E$. In a nonsingular pose of the mechanism the Jacobian $\mathbf{J}$ will have maximal rank. A singular pose is characterized by rank deficiency of $\mathbf{J}$ and the defect is directly related to the local degree of freedom.

In case of the planar 3-$RPR$, the mechanism is in a singular pose whenever the determinant of $\mathbf{J}$ vanishes ($S : \det \mathbf{J} = 0$). Fig. 10 shows the manipulator in a singular pose. It should be noted, that a singular pose has a simple geometric interpretation, namely that the extensions of the three leg lines have to intersect in a point or they are parallel. The equation of $S$ can be written in the form[3]

$$\begin{aligned} S\colon\ & x_0^2(ax_0x_2 + bx_2x_1 + cx_3x_1 + dx_2^2 + ex_3x_2) + x_0x_1[fx_2x_1 + gx_1x_3 + h(x_2^2 + x_3^2)] + \\ & x_1^2(ix_1x_3 + ex_3x_2 - dx_3^2) = 0, \end{aligned} \tag{15}$$

[3]For a more detailed deduction see [12].

where

$$
\begin{aligned}
a &:= (A_3b_3 - B_3a_3)(A_2 - a_2)\\
b &:= 2(-A_2a_2A_3 - a_2A_3a_3 + A_2a_2a_3 + A_2B_3b_3 + A_2A_3a_3 - a_2B_3b_3)\\
c &:= -a_2A_3b_3 + a_2B_3a_3 - 2B_3A_2a_2 + A_2B_3a_3 - A_2A_3b_3 + 2b_3A_2a_2\\
d &:= 2(a_2A_3 - A_2a_3)\\
e &:= 2(a_2B_3 - A_2b_3)\\
f &:= -a_2B_3a_3 + A_2B_3a_3 + a_2A_3b_3 - 2B_3A_2a_2 - A_2A_3b_3 - 2b_3A_2a_2\\
g &:= 2(-A_2A_3a_3 - A_2B_3b_3 + A_2a_2A_3 - a_2B_3b_3 + A_2a_2a_3 - a_2A_3a_3)\\
h &:= 2(a_2B_3 + 2A_2b_3)\\
i &:= (A_3b_3 - B_3a_3)(A_2 + a_2).
\end{aligned}
\tag{16}
$$

This surface is an interesting surface of degree 4. It has been already studied in the $19^{th}$ century by the famous mathematicians A. Clebsch [6] and M. Noether [14]. $S$ has the absolute line of the quasielliptic geometry of the kinematic image space as a double line and because of the double line it is rational. Fig. 11 shows this surface for a generic 3-RPR manipulator. The rational parameterization $(S : x_0 = f_1(u,v), x_1 = f_1(u,v), x_2 = f_2(u,v), x_3 = f_3(u,v))$ has been found in [12] and was used in [11] to map this surface into the joint space. Because of the nonlinearity of the map the surface becomes an algebraic surface $JS$ of degree 12 with a lot of singularities. Fig. 14 shows a horizontal cross section of $JS$. This surface was used to prove that every generic 3-$RPR$ manipulator has the property of non-singular assembly mode change. In Fig. 11 several arcs are displayed. Their end points correspond to different solutions of the direct kinematics i.e. to different poses having the same leg lengths. The curves do not intersect the singularity surface, which means they correspond to a continuous one parameter motion connecting two assemblies without crossing a singularity [11].

Interesting is also the spherical version of the 3-$RPR$ manipulator, which practically is built as 3-$RRR$ manipulator. Kinematically these two versions are the same with the exception of leg singularities when the $RRR$ leg is either folded or fully extended. Figs. 15 and 16 show a working mechanism designed by C. Gosselin, *the Agile Eye*. This manipulator is used for rapid orientation of a camera and has a better and faster orientation capability than the human eye [8]. Using the same approach as with the planar equivalent, one can compute the singularity surface:

$$
\begin{aligned}
&Ax_0^3x_2 + Bx_1^3x_3 + Cx_2^3x_0 + Dx_3^3x_1 + x_0^2(Ex_2x_2 + Fx_1x_3 + Gx_2x_3)\\
&+ x_1^2(Hx_0x_2 + Ix_0x_3 + Jx_2x_3) + x_2^2(Kx_0x_1 + Lx_0x_3 + Mx_1x_3)\\
&+ x_3^2(Nx_0x_1 + Ox_0x_2 + Px_1x_2) + Qx_0^2x_2^2 + Rx_1^2x_3^2 - Sx_0x_1x_2x_3 = 0,
\end{aligned}
\tag{17}
$$

where $A, \dots, S$ are functions of the design parameters (similar to (15)). This degree four surface has the property that it contains all lines of the projective coordinate tetrahedron. It is displayed for a generic choice of the design parameters in Fig. 12. It is conjectured that this surface again has “enough holes” (like the one in the planar manipulator case), so that a non-singular assembly mode change will be possible.

## 5. Conclusion

Compiling results obtained in recent years with special emphasis to geometric objects we have shown that kinematic features yield interesting geometric objects that are worth studying on their own.

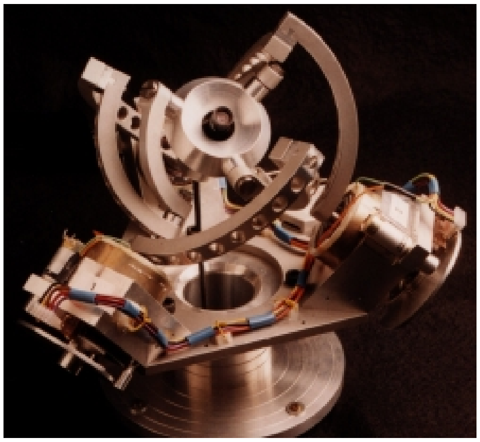

Figure 15: *The Agile Eye* (courtesy Prof. C. Gosselin)

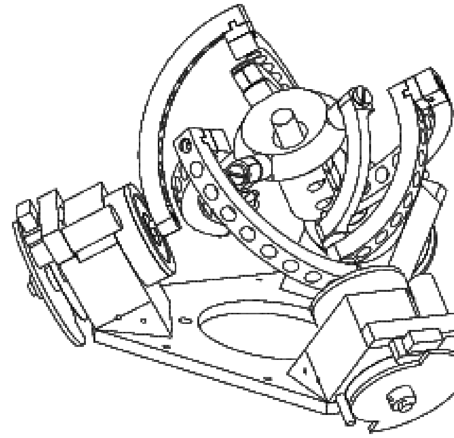

Figure 16: CAD model of *The Agile Eye* (courtesy Prof. C. Gosselin)

## Acknowledgment

H.-P. Schröcker is acknowledged for providing Fig. 10.

## References

[1] W. Blaschke: *Euklidische Kinematik und nichteuklidische Geometrie I, II.* Zeitschr. Math. u. Physik **60**, 61–91 and 203–204 (1911).

[2] W. Blaschke: *Kinematik und Quaternionen.* VEB Verlag, Berlin 1960.

[3] W. Blaschke, H.R. Müller: *Ebene Kinematik.* Oldenburg Verlag, München 1956.

[4] O. Bottema, B. Roth: *Theoretical Kinematics.* Dover Publications, Inc., New York 1990.

[5] M. Ceccarelli: *On the workspace of 3R robot arms.* Proc. 5th IFToMM Int. Symp. on Theory and Practice of Mechanism, Bucharest 1989, Vol. II-1, pp. 37–46.

[6] A. Clebsch: *Über die Abbildung algebraischer Flächen, insbesondere der vierten und fünften Grades.* Math. Annalen **1**, 253–317 (1876).

[7] D.A. Cox, J.B. Little, D. O'Shea: *Ideals, Varieties and Algorithms.* 3rd ed., Springer 2007.

[8] `http://robot.gmc.ulaval.ca/en/research/theme103.html`

[9] J. Grünwald: *Ein Abbildungsprinzip, welches die ebene Geometrie und Kinematik mit der räumlichen Geometrie verknüpft.* Sitzungsber., Abt. II, österr. Akad. Wiss., Math.-Naturw. Kl. **120**, 677-741 (1911).

[10] M.L. Husty: *On the workspace of planar three-legged platforms.* In Proceedings ISRAM – World Congress of Automation, Montpellier/France 1996, pp. 1790–1796.

[11] M.L. Husty: *Non-singular assembly mode change in 3-RPR parallel manipulators.* In A. Kecskeméthy, A. Müller (eds.): *Computational Kinematics,* Proc. of the 5th Intern. Workshop on Computational Kinematics, Springer Verlag 2009, pp. 51–60.

[12] M. Husty, C. Gosselin: *On the singularity surface of planar 3-RPR parallel mechanisms.* Mechanics Based Design of Structures and Machines **36**/4, 411–425 (2008).

[13] M.L. Husty, H.-P. Schröcker: *Nonlinear Computational Geometry.* The IMA Volumes in Mathematics and its Applications, vol. 151, chapter Algebraic geometry and kinematics, Springer 2010, pp. 85–107.

[14] M. Noether: *Über Flächen, welche Schaaren rationaler Kurven besitzen.* Math. Annalen **1**, 161–227 (1876).

[15] E. Ottaviano, M.L. Husty, M. Ceccarelli: *Identification of the workspace boundary of a general 3-R manipulator.* Journal of Mechanical Design **128**(1), 236–242 (2006).

[16] E. Ottaviano, M.L. Husty, M. Ceccarelli: *Level-Set Method for Workspace Analysis of Serial Manipulator.* In *Advances in Robot Kinematics*, Barcelona, Springer, Dordrecht 2006, pp. 307–314.

[17] F. Pernkopf, M.L. Husty: *Workspace classification of Stewart-Gough platforms with planar base and platform.* In J. Lenarčič, C. Galletti (eds.): *On Advances in Robot Kinematics,* Kluwer Acad. Publ. 2004, pp. 229–237.

[18] F. Pernkopf, M.L. Husty: *Workspace analysis of Stewart-Gough-type parallel manipulators.* Journal of Mechanical Engineering Science **220**(7), 1019–1032 (2006).

[19] B. Siciliano, O. Khatib (eds.): *Springer Handbook of Robotics.* Springer Verlag, Heidelberg 2008.

[20] E. Study: *Geometrie der Dynamen.* Teubner Verlag, Leipzig 1903.

Received August 6, 2010; final form May 23, 2012